A COMPUTATIONAL ANALYSIS OF FINITE RATE CHEMICALLY REACTING FLOW BY USING UPWIND N-S METHOD

J. I. Seo, C. O. Kwon and D. J. Song
School of Mechanical Engineering, Yeungnam University
Gyongsan 712-749, Korea

ABSTRACT

A two-dimensional/axisymmetric CSCM upwind flux difference splitting Navier-Stokes method has been developed to study the finite rate chemically reacting invisicd and viscous hypersonic flows over bluntbody. A upwind method was chosen due to its robustness in capturing the strong bow shock waves. For the nonequilibrium chemically reacting air, NS-1 species conservation equations were strongly coupled with flowfield equations through convection and species production terms. The nonequilibrium wall pressure and heat transfer rate distributions along the vehicle were compared with those from equilibrium and perfect gas calculations. The nonequilibrium species distribution shows the reduced concentrations of O and N species when compared with equilibrium species distribution. The solutions resolved strong bow shock waves and heat transfer rate very accurately when compared with central difference schemes.

1. INTRODUCTION

Nonequilibrium chemically reacting gas flow has been a very important research area due to recent interests in successive planet exploration missions. Hypersonic flows are usually characterized by strong bow shocks, high temperature and low density. Accurate prediction of these effects is critical to the design hypersonic vehicles.

Developments of new and powerful computers and algorithms have enabled the analysis of hypersonic flow over realistic entry vehicles coupled nonequilibrium chemistry Navier-Stokes codes. Some of the most important algorithm advances for the computation of hypersonic flows have been in the development of upwind and non-oscillatory schemes (Van Leer(1979) and Roe(1981)). Upwind flux vector splitting and upwind flux difference splitting methods have been extended by various researchers (Vinokur(1988), etc.). In this study we developed chemically nonequilibrium upwind flux difference splitting Navier-Stokes method of Lombard et al.(1982) to study the finite rate chemically reacting inviscid and viscous hypersonic flows over bluntbody. High temperature effects are studied by comparing surface measurable quantities among different gas models.

2. ANALYSIS

2.1. Conservative Supra Characteristic Method

The CSCM flux difference splitting algorithm of Lombard et al.(1982) and Widhopf and Wang's(1988) coupling algorithm have been applied to include a fully coupled nonequilibrium chemistry.

2.1.1. *Governing equations*

A finite difference formulation of the compressible Navier-Stokes equations for axisymmetric flow can be expressed for general difference operators in general curvilinear coordinates in the form

$$\begin{aligned} & \frac{1}{J}\frac{\partial q}{\partial \tau} + \frac{\partial}{\partial \xi}\left(\frac{\xi_x}{J}f + \frac{\xi_y}{J\bar{y}}yg\right) + \frac{\partial}{\partial \eta}\left(\frac{\eta_x}{J}f + \frac{\eta_y}{J\bar{y}}yg\right) \\ = \quad & \frac{1}{J}\delta_\tau q + \Delta_\xi F + \Delta_\eta G \qquad (1) \\ = \quad & \Delta_\xi\left(\frac{\xi_x}{J}f_v + \frac{\xi_y}{J\bar{y}}yg_v\right) + \Delta_\eta\left(\frac{\eta_x}{J}f_v + \frac{\eta_y}{J\bar{y}}yg_v\right) \\ & + \frac{1}{J}S \end{aligned}$$

The inviscid flux f , viscous flux f_v, conservative dependent variables q and source term S are given in terms of the usual primitive variables by

$$q = \begin{pmatrix} \rho \\ \rho u \\ \rho v \\ \varepsilon \\ \rho_i \end{pmatrix}, \quad f = \begin{pmatrix} \rho u \\ \rho u^2 + p \\ \rho uv \\ u(\varepsilon + p) \\ \rho_i u \end{pmatrix}, \quad S = \begin{pmatrix} 0 \\ 0 \\ 0 \\ 0 \\ \dot{\omega}_i \end{pmatrix} \qquad (2)$$

$$f_v = \begin{pmatrix} 0 \\ \tau_{xx} \\ \tau_{xy} \\ u\tau_{xx} + v\tau_{xy} + k\frac{\partial T}{\partial x} + \sum_{i=1}^{ns} \rho h_i D_{im} \frac{\partial c_i}{\partial x} \\ \rho h_i D_{im} \frac{\partial c_i}{\partial x} \end{pmatrix} \quad (3)$$

where the volumetric total energy $\epsilon = \frac{p}{(\gamma-1)} + \frac{1}{2}\rho(u^2 + v^2)$.

2.1.2. *CSCM formulation*

The CSCM upwind flux difference splitting method utilizes the properties of similarity transformation based on the conservative(q), the primitive($\tilde{q}$) and the characteristic variables($\tilde{\tilde{q}}$)

$$\begin{aligned} \partial_\xi F &= A\partial_\xi q = MT\Lambda T^{-1}M^{-1}\partial_\xi q \quad (4) \\ &= MT\Lambda T^{-1}\partial_x \tilde{q} = MA'\partial_x \tilde{q} \\ &= MT\Lambda\partial_x \tilde{\tilde{q}} \end{aligned}$$

where Λ is a diagonal matrix whose diagonal elements correspond to the eigenvalues.
M matrix transforms primitive variables $\tilde{q}$ into conservative variables q. T^{-1} is a matrix which transforms primitive variables into characteristic variables. The inviscid flux ΔF can be divided into ΔF^+ and ΔF^- using diagonal truth function matrix $D^\pm$ and Eq.(4) can be written as

$$\begin{aligned} \Delta\widehat{F} &= MTIT^{-1}A'\Delta\tilde{q} \\ &= MT(D^+ + D^-)T^{-1}A'\Delta\tilde{q} = \Delta\widehat{F}^+ + \Delta\widehat{F}^- \end{aligned}$$

Using the relation $A'\Delta\tilde{q} = \widetilde{M}^{-1}\Delta q$, the above equation can be rewritten as

$$\Delta\widehat{F}^\pm = MTD^\pm T^{-1}\widetilde{M}^{-1}\Delta q = A^\pm \Delta q \quad (5)$$

Eq.(5) satisfies the property 'U' of Roe and thus the fluxes are conserved.

The implicit finite difference equation can be discretized using one side differencing depending on the sign of eigenvalues of the jacobian matrices and are solved along ξ-direction and then η-direction successively(Diagonal Dominance ADI procedure).

$$\begin{aligned} &\left(-A^+, X, A^-\right) X^{-1} \left(-B^+, X, B^-\right) \delta q = RHS \\ &\left(-A^+, X, A^-\right) \delta q* = RHS \\ &\left(-B^+, X, B^-\right) \delta q = X\delta q* \\ &q^{n+1} = q^n + \Delta q \end{aligned}$$

where $X = I + A^+ - A^- + B^+ - B^-$, and B represent Jacobian matrix of G.

2.1.3. *Reaction model*

We described chemical reaction using the Blottner's(1971) 5 species - 17 reaction equation model.

2.1.4. *Thermodynamic relations*

The pressure, temperature and the parameter γ are related with the dependent variables through the equation of state (with *Dalton's Law*)

$$p = \rho\frac{R_u}{M}T \equiv \sum_{i=1}^{NS}\frac{\rho_i}{M_i}R_u T \quad (6)$$

where $\rho_{NS} = \rho - \sum_{i=1}^{NS-1}\rho_i$ and a volumetric internal energy relation

$$P = \rho e = \sum_{i=1}^{NS}\rho_i e_i \ , \ e = \frac{1}{\gamma - 1}\frac{p}{\rho} \quad (7)$$

The specific internal energy of each species is given by table(Browne,1962). The frozen specific enthalpy of the mixture is determined by summing the individual contributions of each species from the data table as

$$h = \sum_{i=1}^{NS} C_i h_i \ , \ h_i = \int_{T=293K}^{T} c_{p_i} dT + \Delta h_i^F \quad (8)$$

where C_i is the concentration of species i.

2.1.5. *Temperature equations*

The temperature of the nonequilibrium gas mixture can be obtained from the equation of state of thermally perfect but calorically imperfect gas using the Newton-Raphson method around T^k

$$T^{k+1} = T^k - \frac{g(T^k) - e}{g'(T^k)} \quad (9)$$

$$g(T^k) = \sum_{i=1}^{NS} C_i \left(h_i(T) - RT/M_i\right) \quad (10)$$

$$g'(T^k) = \sum_{i=1}^{NS} C_i \left(c_{p_i}(T) - R/M_i\right) \quad (11)$$

and k indicates the iteration index. Then at a given T, take Eqs.(7) and (8) as the basis for defining the ratio of frozen mixture enthalpy to specific internal energy, $\gamma = h/e$.

2.2. Transport Properties and Diffusion Models

Transport properties are required to describe the diffusion of mass, momentum, and energy in gas. Thermochemical equilibrium flow most often use curve fits for μ and k as a function of temperature and pressure. Transport properties in chemically nonequilibrium flows are defined as functions of constituent species transport properties and respective mole fractions

in the mixture. Individual species transport properties are readily available in the form of curve fits as functions of temperature. In this study, mixing rules for viscosities and thermal conductivities are based on Wilke's semi-empirical mixing rule. And for simplicity, we used binary diffusion model defined by Lewis number of 1.4 .

2.3. Stiffness

Due to stiffness problem in chemical reaction source term, fluid mechanics terms and source terms are fully coupled using Widhopf and Wang's algorithm.

2.4. Boundary Conditions

At boundaries we use fully coupled implicit approximations based on the characteristic relations for characteristics running toward the boundaries from the interior. Specially, the boundary conditions used in axisymmetric nonequilibrium chemically reacting flows over bluntbody are supersonic inflow and super sonic outflow conditions. They are defined as

- Inflow : 8 physical boundary conditions, i.e. global density, 4 species density, total energy and flow direction
- Outflow : 8 numerical boundary conditions using $0th$ order extrapolations
- Center line : axisymmetric boundary conditions
- Wall : slip(inviscid), no-slip(viscous) conditions, non-catalytic(inviscid), catalytic(viscous) conditions, adiabatic(inviscid), isothermal(viscous) conditions

3. RESULTS AND DISCUSSION

The new coupled CSCM upwind Navier-Stokes method has been developed to study the hypersonic nonequilibrium(NQ) flow characteristics over a 5° sphere-cone vehicle. The nose radius of sphere-cone vehicle is $0.0254m$ and the vehicle is 4 nose radii long. Figure 1 shows the comparison of wall pressure distribution among the perfect gas(PG), the equilibrium(EQ) air, the NQ air CSCM and the EQ air VSL method at Mach 15 and altitude of 30km. The high pressure at stagnation point is rapidly expanded around the sphere. The predicted wall pressure values from all models are almost the same. Pressure is found to be generally less sensitive to the choice of gas model, because it is a momentum variable and less influenced by the thermodynamic state of the gas.

Figure 2 shows the pressure contour plot from NQ air at Mach 20 and altitude of 30km. Due to roubustness of CSCM upwind method, the strong bow shock in front of blunt nose is sharply captured without any oscillation.

Figure 3 shows the comparison of pressure and temperature profiles along the stagnation streamline between EQ and NQ models. NQ shock thickness is a little bit thicker about one grid point than EQ shock thickness and temperature is higher than that of EQ air. At EQ flow, the shock temperature is adapted to proper EQ shock value instantaneously through endothermic process. At this flight condition, the difference between EQ and NQ flow is rather small. However, for the higher altitude hypersonic flight conditions, the characteristic reaction time is much longer than the characteristic flow time, thus the flow is essentially in chemically nonequilibrium condition.

Figure 4 shows the comparison of pressure and temperature along the stagnation streamline among different air models at Mach 20 and altitude of 50km. The NQ chemistry effect can be clearly seen in this figure. As shown, the differences in shock stand-off distance are apparent among three gas models compared to Fig.3. The largest shock stand-off distance occurs with the PG gas models, whereas the shortest one occurs with the EQ air model. Since the PG density ratio across the shock can not be over 6 by Rankine-Hugoniot relations, the shock stand off distance is larger than any other models to satisfy the mass conservation. The different gas models produce the substantially different maximum temperature profiles along the stagnation streamline.

The species mass fraction comparison between EQ and NQ flow along the stagnation streamline at Mach 20 and altitude of 50km is given in Fig. 5. Since the shock layer temperature is high, the most part of O_2 species is dissociated. The mass fraction of N and O are increased in accordance with the level of dissociation of O_2 and N_2. For EQ air, the reactions are occurred rapidly when compared to NQ air.

Figure 6 (a) and (b)show the comparison of temperature contour between CSCM EQ and CSCM NQ inviscid flow at Mach 20 and altitude of 50km respectively. For NQ air, the temperature near the shock is higher than that of EQ air model and these differences are apparent over entire flow-field.

Figure 7 shows the comparison of pressure and heat transfer rate distributions along the wall between CSCM and VSL methods for NQ viscous flow at Mach 15 and altitude of 60km. The wall temperature was fixed at 1111K. The predicted pressure and heat transfer rate values from current Navier-Stokes methods are in excellent agreement with that of the VSL method.

4. CONCLUSIONS

A two-dimensional/axisymmetric finite-rate chemically reacting CSCM upwind flux difference splitting Navier-Stokes method has been developed to study the

invisicd and viscous hypersonic flows over bluntbody. Peak temperature and shock-layer thickness are substantially reduced with EQ and NQ air models. The PG and the EQ air models show the upper or lower limits of various physical properties compared with NQ air model at low density nonequilibrium hypersonic flow condition. The current Navier-Stokes method with coupled finite-rate chemistry described the nonequilibrium effects in hypersonic flowfield resonably.

REFERENCES

Blottner, F. G., Johnson, M. and Ellis, M.(1971) Chemically Reacting Viscous Flow Program for Multi-Component GAS Mixtures, Sandia Lab., Report No. SC-RR-70-754.

Browne, W.G.(1962) Thermodynamics properties of Some Atoms and Atomic Ions, MSD Engineering Physics TM3, General Electric Co., Philadelphia,PA.

Lombard, C. K.(1982) Conservative Supra-Characteristic Method for Splitting the Hyperbolic Systems of Gasdynamics for Real and Perfect Gases, NASA CR-166307.

Roe, P. L.(1981) Approximate Riemann Solvers, Parameter Vectors, and Difference Scheme, Journal of Computational Physics, Vol. 43, pp.357-372

Vinokur, M.(1988) NASA CR-177512

Van Leer, B.(1979), Towards the Ultimate Conservation Scheme: A Second-Order Sequel to Godonov's Method. Journal of Computational Physics, Vol. 32, pp. 101-136.

Widhopf, G. F. and Wang, J.C.T.(1988) A TVD Finite-Volumn Technique for Nonequilibrium Chemically-Reacting Flows, AIAA-88-2711.

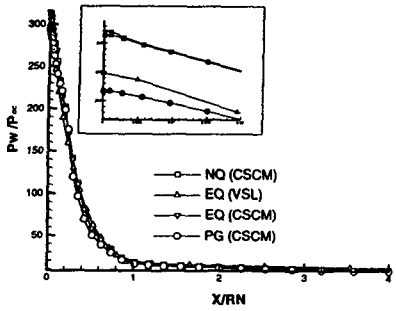

Fig.1 Comparison of wall pressure distribution along the surface among different gas models at M=15 and altitude of 30km

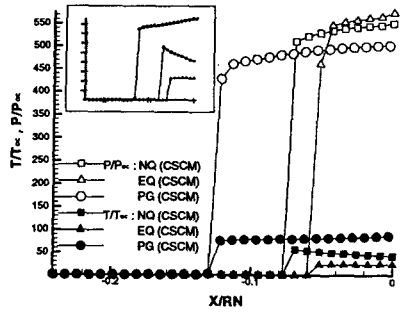

Fig.4 Comparison pressure and temperature profiles along the stagnation streamline among different gas models at M=20 and altitude of 50km

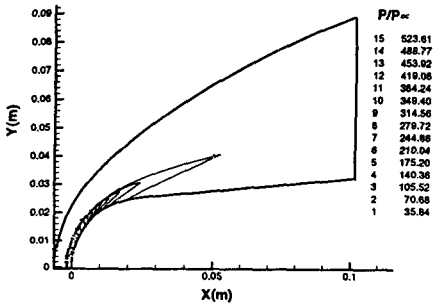

Fig.2 Pressure contour plot over the blunted vehicle from non-equilibrium air at M=20 and altitude of 30km

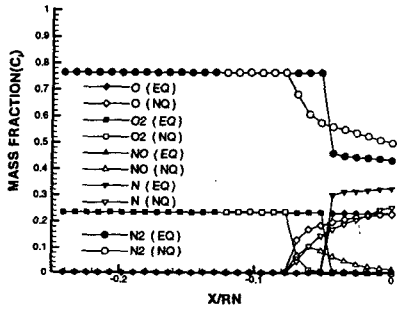

Fig.5 Comparison of 5species mass fraction distribution along the stagnation streamline between equilibrium and non-equilibrium flow at M=20 and altitude of 50km

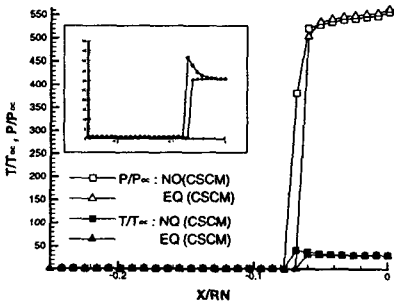

Fig.3 Comparison of pressure and temperature profiles along the stagnation streamline between equilibrium and non-equilibrium flow at M=20 and altitude of 30km

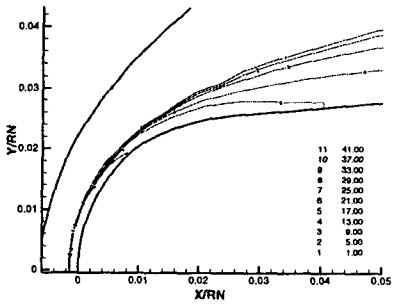

(a)

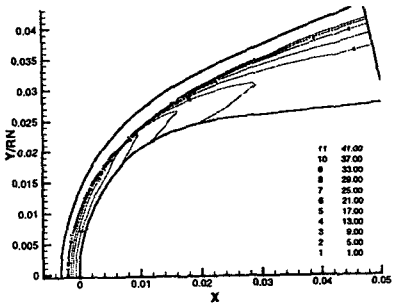

(b)

Fig.6 Temperature contour plot comparison between (a)equilibrium and (b) non-equilibrium air model at M=20 and altitude of 50km

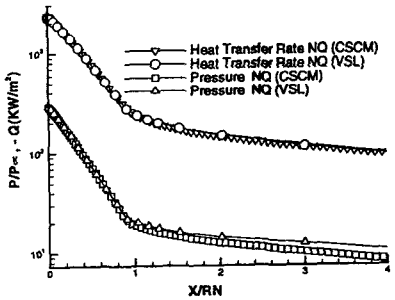

Fig.6 Comparison of pressure and heat transfer rate distributions along the wall between CSCM and VSL non-equilibrium viscous flow at M=15 and altitude of 60km